Construction and Building Materials 167 (2018) 707–715

Contents lists available at ScienceDirect

Construction and Building Materials

journal homepage: www.elsevier.com/locate/conbuildmat

Investigating the impact of different loading patterns on the permanent deformation behaviour in hot mix asphalt

Seyed Mohsen Motevalizadeh [a,*], Pooyan Ayar [b], Seyed Hossein Motevalizadeh [c], Sadegh Yeganeh [d], Mahmoud Ameri [d], Keyvan bemana [d]

[a] School of Civil Engineering, Tarbiat Modares University (TMU), Tehran, Iran
[b] Escuela Técnica Superior de Ingeniería de Caminos, Canales y Puertos, Campus Universitario Fuentenueva, Universidad de Granada, C/Severo Ochoa s/n 18071, Granada, Spain
[c] School of Civil Engineering, Science and Research Branch of Tehran, Azad University, Tehran, Iran
[d] School of Civil Engineering, Iran University of Science and Technology, Tehran, Iran

HIGHLIGHTS

- Permanent deformation depends on the loading patterns and testing parameters.
- Power-law model can be used to analyze the permanent deformation characteristic.
- An increase in rest period and loading duration leads to a higher permanent deformation.

ARTICLE INFO

Article history:
Received 20 September 2017
Received in revised form 8 February 2018
Accepted 9 February 2018
Available online 22 February 2018

Keywords:
Permanent deformation
Power-law model
Cyclic loading
Repeated Loading Permanent Deformation (RLPD) test
Loading pattern
Flow number

ABSTRACT

This research was conducted to evaluate the effect of different loading combinations on the permanent deformation behaviour in asphalt mixtures. Therefore, repeated loading permanent deformation test was performed considering different stress levels, loading durations, rest periods and testing temperatures. The results showed that the slope coefficient of Power-law model has a more influence on permanent deformation compared to intercept. Moreover, rutting zones are sensitive to testing parameters. Rest period could significantly affect the first zone. Nevertheless, secondary zone depends on the loading duration and deviator stress. Eventually, the testing temperature has the greatest influence on the permanent deformation behaviour.

1. Introduction

Permanent deformation in Hot Mix Asphalt (HMA) occurs predominantly at higher temperatures [1]. This distress mostly occurs in the upper layers than the subgrade when the traffic volume, tire pressure and axle loads are increased [2]. Development of permanent deformations reduce the service life of asphalt pavements. Furthermore, this distress could decrease the level of safety in road transportation networks [3].

Various laboratory tests have been introduced to study the resistance of HMA against permanent deformations [3–7]. Accordingly, the development of permanent deformation models is useful to predict the response of asphalt layers under traffic loading [8].

Among different test methods, NCHRP Project 9–19 [9] has assessed Flow Time (FT), Flow Number (FN) and Dynamic Modulus (|E∗|) in order to determine a simple performance test to study the permanent deformation resistance in asphalt mixtures. According to these test methods, researchers found that the FN could be considered as a better method to evaluate the rutting resistance of HMA [4,10–12]. In addition, Faheem et al. [13] indicated that the FN is one of the most important characteristics of HMA, which has a considerable correlation with Traffic Force Index (TFI). This index shows the density of traffic during service life of asphalt pavements. Nowadays, the FN that can be obtained from Repeated Loading Permanent Deformation (RLPD) test is widely employed as an accelerated performance test by different researchers [12,14].

* Corresponding author.
E-mail addresses: mohsen.motevalizadeh@modares.ac.ir (S.M. Motevalizadeh), payar@correo.ugr.es (P. Ayar).

https://doi.org/10.1016/j.conbuildmat.2018.02.049
0950-0618/

The RLPD test is widely used to assess the permanent deformation characteristics of HMA since it was utilized by Monismith et al. [15] in the mid-1970. Generally, in this test method a dynamic compressive loading pulse at high temperature conditions is applied to cylindrical specimens until their failure point (i.e. FN number). [8,12,16,17]. During this test, the accumulated permanent deformation is recorded as a function of loading cycles (Fig. 1).

The accumulated permanent strain includes three different zones: primary, secondary and tertiary [8,12,18–20]. In primary zone, the accumulated permanent deformation grows rapidly until reaches the onset of secondary zone. Upon starting the secondary zone, the rate of permanent strain per cycle is reduced to achieve a constant value. In this stage, the accumulated permanent deformation grows as a linear equation until the start of the tertiary zone. In the third stage, the accumulated permanent deformation per loading cycles begins to increase rapidly until the failure in the material reaches. The starting point of this stage is called as FN [1,9,21]. As it was mentioned previously, the FN value has been recommended as a rutting resistance indicator for HMA [8].

Selecting the parameters of RLPD test can be considered as one of ambiguous points in this procedure. In this regards, Table 1

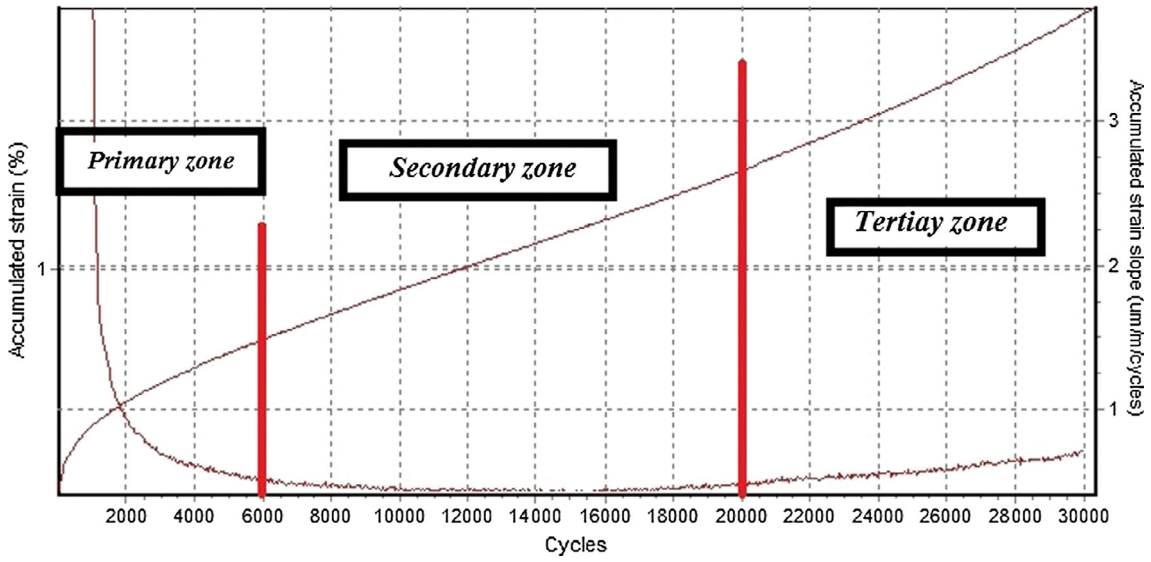

Fig. 1. Typical relationship between accumulated permanent strain, accumulated strain slope and number of cycles under a RLPD test.

Table 1
Parameters employed by previous researchers in RLPD test. (See below-mentioned references for further information.)

	Test type	Temperature	Confining pressure	Deviator stress	Loading pattern	References
NCHRP Project 9-19	Unconfined RLPD test	54 °C	0	70 - 210 kPa	Haversine waveform, 0.1 s loading duration and 0.9 s rest period	[12], [22]
	Confined RLPD test	54 °C	35 – 210 kPa	490-980 kPa		[23]
NCHRP Project 9-33	Unconfined RLPD test	-	0	600 kPa		[24]
NCHRP Project 9-30A	Confined RLPD test	-	69 kPa	483 kPa		[25]
NCHRP Project 673	Unconfined RLPD test	-	0	600 kPa		[12]
NCHRP Project 719	Confined RLPD test	-	69 kPa	482 kPa		[12]
Kaloush et al.	Unconfined RLPD test	37.8 and 57.4	0	68.9, 137.9 and 206.8 kPa		[26]
Zhou et al.	Unconfined RLPD test	40	0	138 kPa		[8]
Biligiri et al.	Unconfined RLPD test	40	0	600 kPa		[27]
Ameri et al.	Unconfined RLPD test	45	0	200 kPa		[28]
Qi et al.	Unconfined RLPD test	38 and 55 C	0	69 and 137 kPa	Loading duration: 0.1, 10 and 1000 second Rest period: 0.9, 10 and 1000 second	[3]
Australian: AS 2891.12.1	Unconfined RLPD test	-	0	200	Square pulse using 0.5 s loading duration and 1.5 s rest time	[29]
British: DD 226	Unconfined RLPD test	-	0	100	Square pulse using 1 s loading duration and 1 s rest time	[30]
European: pr EN 12697	Unconfined RLPD test	-	0	100	Square pulse using 1 s loading duration and 1 s rest time	[31]
VESYS manual	Unconfined RLPD test	-	0	138	Haversine pulse using 0.1s loading duration and 0.9 s rest time	[32]

presents different parameters employed by previous researchers to apply RLPD test. The selection of these parameters may play an important role in the study of permanent deformation in HMA.

Fig. 2a illustrates the duration of loading and rest period in multi-cycle loading/unloading process under haversine waveform. The haversine waveform as the most suitable waveform in order to simulate traffic loading has been recommended by previous researchers [2,3]. Fig. 2b shows the accumulated permanent strain in HMA under cyclic loading. By considering the strain components, the compressive loading waveform has significant impact on the permanent deformation of HMA. Fig. 2c shows strain components of a viscoelastic material under haversine loading, which include loading duration (t_l) and rest time (t_d). In this respect, Qi et al. [3] stated that creep curve of HMA under a single compressive load cycle comprises four components including elastic strain, plastic strain, visco-elastic strain and visco-plastic strain. The immediate strain (ε_0) contains an elastic (ε_e) and a plastic (ε_p) parts as well as two viscose contents. According to the visco-elasto-plastic behaviour of HMA, the elastic strain instantly rebounds after unloading. Subsequently, the visco-elastic component of the strain reverts over the time. In general, elastic and viscoelastic forms of the resilient and the plastic strains constitute the permanent strain.

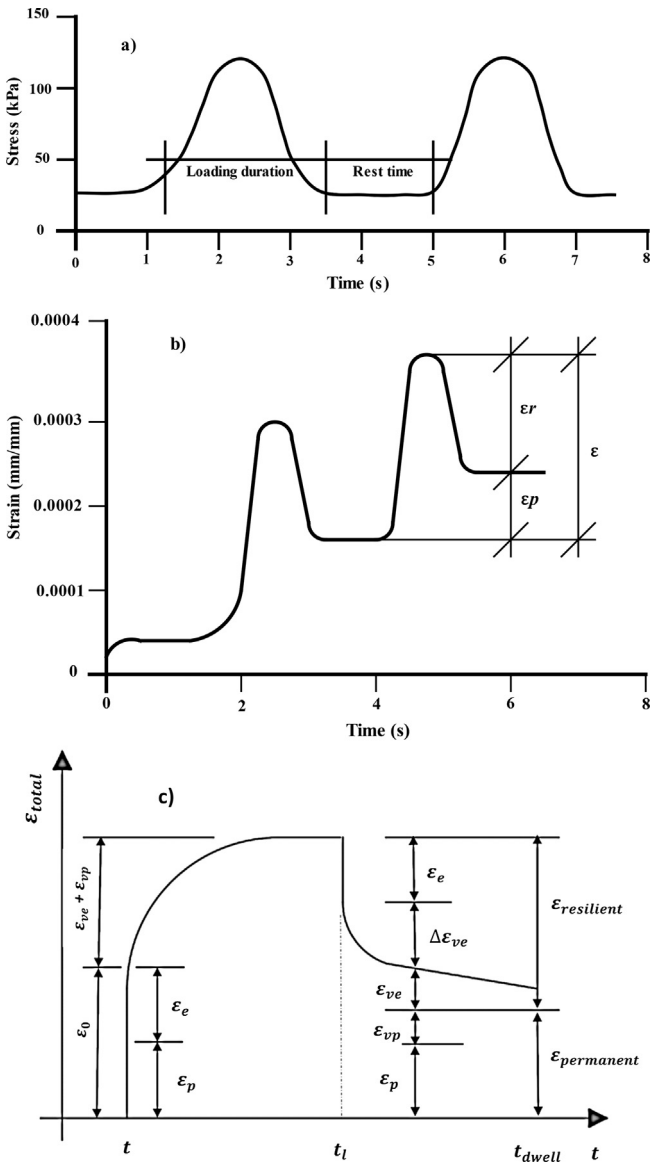

Fig. 2. (a) The loading duration and rest time in RLPD test, (b) total strain in HMA under repeated loading and (c) strain components under haversine loading.

2. Predictive models for permanent deformation of HMA

In recent years, different models have been suggested to investigate and predict the permanent deformation characteristics of HMA under cyclic loading (Table 2). Based on previous researches, it can be stated that the Power-law model is an appropriate model to study the permanent deformation resistance of HMA [3]. More information on Power-law model provided below.

Both the Semi-log and Power-law models are widely used to represent the primary stage of creep curve [8]. Nevertheless, Qi et al. [3] indicated that the empirical linear equation $\log(\varepsilon_p - \log N)$ is the most appropriate statistical model to describe the permanent deformation behaviour of HMA. This model has been presented in Eq. (1). When the logarithmic form is considered, Eq. (1) can be changed to Eq. (2):

$$\varepsilon_p = aN^b \tag{1}$$

$$\log \varepsilon_p = \log a + b \times \log N \tag{2}$$

where (a) and (b) are expressed the characteristics of the permanent deformation of HMA under cyclic loading. Some investigators reported that the Eq. (1) could not be utilized to describe the tertiary stage. For this purpose, model coefficients can be determined using multiple regression approach [3]. The developed model has been presented in Eq. (3).

$$\varepsilon_p = a(t_l, t_d, T, \sigma) \times N^{b(t_l, t_d, T, \sigma)} \tag{3}$$

where ε_p is accumulated permanent strain; t_l is loading duration; t_d is rest time; T is temperature (°C); σ is stress level; N is number of load repetition; a is intercept as a function of t_l, t_d, T and σ and b is slope as a function of t_l, t_d, T and σ.

In order to develop Power-law model's coefficients that mentioned in Eq. (3), Qi et al. [3] employed three types of mathematical equations, including linear, semi-log and exponential. They stated that the Eqs. (4) and (5) can be considered as more suitable equations to predict intercept and slope of Power-law model.

$$Y = A_0 \times X_1^{A1} \times X_2^{A2} \times \ldots \tag{4}$$

$$Y = A_0 + A_1 \times \log X_1 + A_2 \times \log X_2 + \ldots \tag{5}$$

where $A_0, A_1, A_2, \ldots$ are the model coefficients that should be calculated using multiple regression method and $X_1, X_2, X_3, \ldots$ are the model's parameters.

Regardless of the mixture types, loading conditions affect the permanent deformation of HMA during secondary zone. In addition, a statistical model can be used to have a better image from the impact of loading parameters. As mentioned previously, the Power-law model was suggested as a powerful model to predict the permanent deformation characteristic. Nevertheless, the influence of experimental parameters on model coefficients and predictive permanent deformation should be clarified. Therefore, introducing a predictive model that its coefficients are function of experimental parameters can lead to a more accurate evaluation of permanent deformation.

3. Objectives

The main objective of this research is to find an experimental model in order to predict the permanent deformation behaviour

Table 2
Details of the predictive models for permanent deformation in asphalt mixtures.

Name	Permanent Deformation Model	Variables	Comments
Semi-log model [33]	$\varepsilon_p = a_1 + b_1 \times \log(N)$	ε_p: Accumulated permanent strain N: Number of cycle, a_1 and b_1: Regression coefficient	This method is used only to assess the primary and secondary zones in creep curve
Power model [15]	$\varepsilon_p = aN^b$	ε_p: Accumulated permanent strain N: Number of cycle, an and b: Regression coefficient	This method is used only to assess the primary and secondary zones and the parameters depend on the material characterization and testing conditions
Vesys model [34]	$\varepsilon_{pn} = \mu_0 eN^{-\alpha}$	ε_{pn}: Accumulated permanent strain at each loading cycle, e: Maximum strain under a haversine loading wave regarding to 0.1 s loading duration, α=1-S, S: Secondary zone slope of creep curve I: Intercept of creep curve, μ_0:$\frac{IS}{e}$	This model is based on the Vesys approach and its parameters obtained from RLPD test
Bayomy model [35]	$\text{pre} - \text{failurezone} : \varepsilon_p = A_1 e^{b_1 N}$ Failurezone : $\varepsilon_p = aN^b$	ε_p: Permanent strain, N: Load of cycle, A1, b1, an and b: Regression coefficient	This model is based on the results of RLPD test.
Tseng & Lytton model [36]	$\varepsilon_{pa} = e_0 \times e^{-(\rho/N)^\beta}$	ε_a: Permanent strain, N: Load of cycle, e_0, ρ and β: Regression coefficient	This model is based on the RLPD test results
AASHTO 2002 model [37]	$\log\frac{\varepsilon_p}{\varepsilon_r} = \log(c) + 0.4262 \times \log(N)$	$\varepsilon_p, \varepsilon_r$: Permanent and resilient strain, respectively, N: Load of cycle, c: Regression coefficient	–
Kaloush and Witczak model [9]	$RD_{23} = a \times ESAL^b + C \times (e^{d \times ESAL} - 1)$	ESAL: Equivalent single axle load, a, b and d: Regression coefficient, $C = T^{\left(\frac{2.02755}{5615.391}\right)}$: Function of temperature (°F)	–
FNest model [38]	$\varepsilon_p = \frac{1}{\beta}[-\ln(1 - \frac{N}{\gamma}]^{1/\alpha})$ $FN = \gamma[1 - \exp(\frac{1}{\alpha} - 1)]$	ε_p: Permanent strain, N: Load of cycle, α, β and γ: Regression coefficient, FN: Flow number	This model is used to determine the onset of tertiary zone based on the RLPD test results
Francken model [27]	$\varepsilon_p(N) = AN^B + C(e^{DN} - 1)$	$\varepsilon_p(N)$: Permanent strain, N: Load of cycle, A, B,C and D: Regression coefficient	This model is based on the RLPD test results, considering different stress levels and temperatures This model assess all three stages in creep curve
Hoerl model [39]	$\frac{d\varepsilon_p}{dN} = (A \times B^N \times N^C)$	$\varepsilon_p(N)$: Permanent strain, N: Load of cycle, A, B,C and D: Regression coefficient	This model assess all three stages in creep curve using RLPD test results

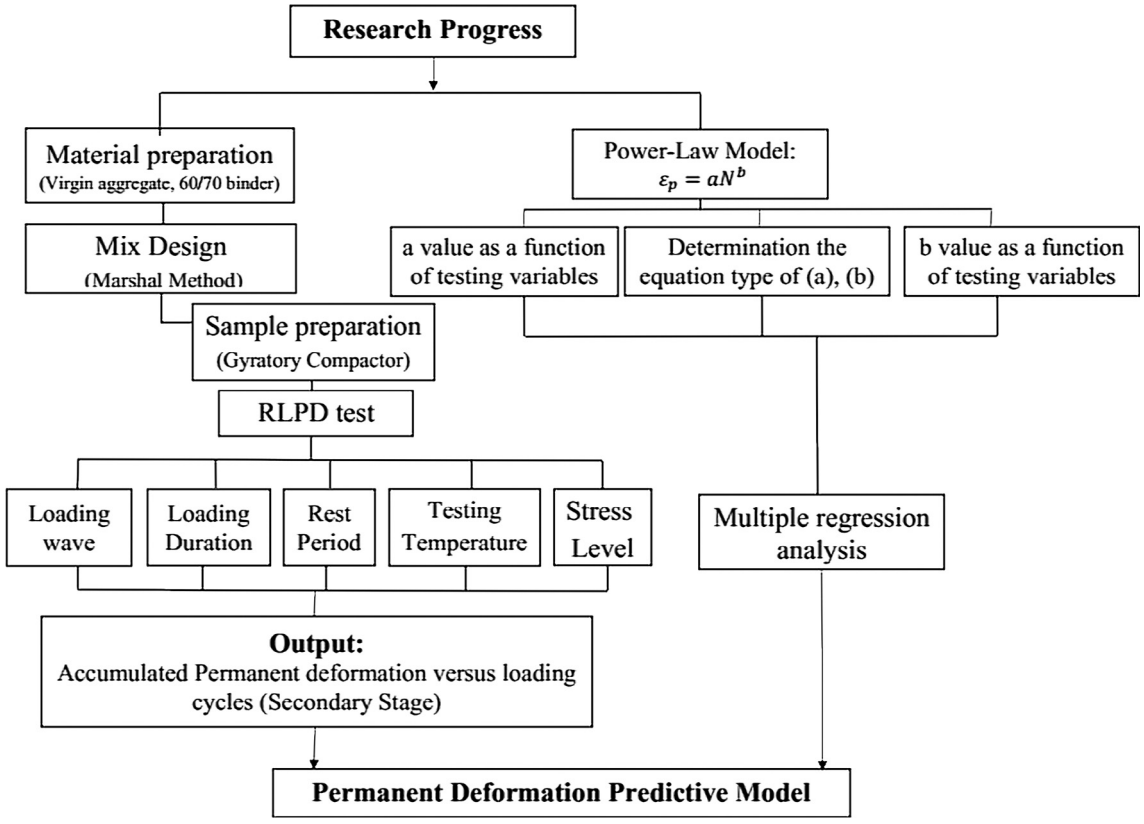

Fig. 3. Outline of the experimental and analytical procedures used in this study.

of HMA. Furthermore, the impact of experimental variables on the permanent deformation of HMA was investigated. To this end, different testing variables including rest period, loading duration, stress level and temperature were selected to study this behaviour using RLPD test under different loading conditions. In this respect, Fig. 3 summarizes the experimental and analytical procedure of this research.

4. Experimental design

4.1. Materials

Aggregates used in this research were prepared from crushed limestone. The aggregate gradation curve was selected according to Iran Highway Asphalt Paving Code and it is illustrated in Fig. 4 [40]. Some physical and mechanical properties of aggregates have been presented Table 3. Additionally, the unmodified 60/70 penetration grade bitumen was used to prepare the specimens. The basic properties of bitumen have been shown in Table 4. According to Marshall mix design [41], the optimum binder content was fixed to 5% by total mass of the mix. The Superpave Gyratory Compactor (SGC) was employed to fabricate the 4-inch diameter cylindrical specimens (Table 5).

Table 4
Physical properties of the binder.

Parameter	Value	Unit	Method
Penetration at 25 °C	64	0.1 mm	ASTM D5
Softening point (R&B)	50.6	°C	ASTM D36
Ductility at 25 °C	>100	Cm	ASTM D113
Flash and fire point	308	°C	ASTM D92
Specified gravity at 25 °C	1.0296	g/cm3	ASTM D70

Table 5
The settings of SGC device.

Factor	Value
Angle of tilt	1.25°
Loading ram	600 Kpa
Rotation speed	90 rpm
Specimen height	68 mm

4.2. Methods

The Universal Testing Machine (UTM-5) equipped with temperature control chamber (Fig. 5) was utilized to perform the RLPD test. Furthermore, in order to study the impacts of loading

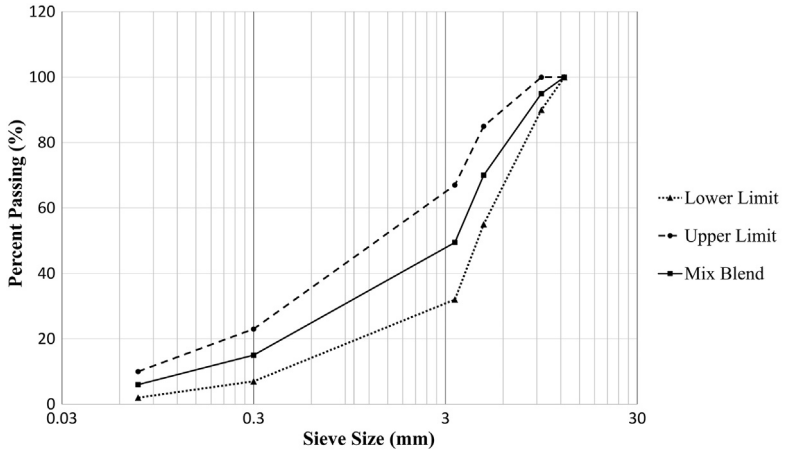

Fig. 4. The aggregate gradation used in this study.

Table 3
Physical properties of aggregates.

Property		Value			Limits
		Coarse aggregate	Fine aggregate	Filler	
Specific Gravity (gr/cm^3) (ASTM C 127 & 128)	–	2.523	2.486	2.578	–
Sand Equivalent (SE)	–	–	73	–	Min. 50
Fine Aggregate Angularity (AASHTO TP33)	–	–	47	–	Min. 45
Los Angeles Abrasion Value (AASHTO T96)	Number of Rotation	500	–	–	–
	Abrasion value	14.4	–	–	Max. 30
Atterburg Limits (AASHTO T89, T90)	Plasticity Index	–	N.A.	2	Non-plastic
	Plastic Limit (PL)	–	0	22	–
	Liquid Limit (LL)	–	N.A.	24	–
Percentage of Fractured Particles in Coarse Aggregate (ASTM D5821)	One Side	100	–	–	Min. 100
	Two Side	92	–	–	Min. 90
Flakiness and Elongation (BS 812)	Elongation	19.4	–	–	Max. 20
	Flakiness	3.1	–	–	Max. 5
Soundness of Aggregate by Use of Sodium Sulphate or Magnesium Sulphate (AASHTO T104)		0.94	2.8	–	

Fig. 5. UTM-5 apparatus equipped with temperature control chamber.

Table 6
Loading patterns used in this research.

Parameter	Value			Unit
Loading time	100	500	1000	ms
Rest ratio (Rest time/loading time)	1/1		1/9	–
Stress level	100		200	kPa
Temperature	40		55	°C
Loading wave		Haversine		
Replicate		2		–

(i.e. traffic density and axle weight) and environmental conditions on permanent deformation behaviour, different experimental parameters such as loading duration, rest time, stress level and testing temperature were considered in this research. Based on testing protocols that suggested by international codes (Table 1), the selected parameters to conduct RLPD test in this study have been presented in Table 6.

5. Results and discussion

A statistical method was employed to develop a model to analyse the rutting behaviour in HMA under cyclic loading, considering different testing conditions. It can be seen from Fig. 6 that the majority of samples cannot reach to the onset of the tertiary zone under different testing conditions (this could be due to applying low levels of stress). Therefore, the rutting resistance of HMA in primary and secondary stages has been analysed. Furthermore, the Power-law model was selected to study the creep curve under cyclic loading in this research. In order to analyse the impact of different variables, intercept and slope of the Power-law model were defined as a function of testing parameters. Accordingly, Eqs. (6) and (7) were selected to predict the coefficients of the model.

$$a = a_1 \times T^{\alpha_1} \times S^{\alpha_2} \times L^{\alpha_3} \times R^{\alpha_4} \tag{6}$$

$$b = b_1 + \beta_1 \times \log T + \beta_2 \times \log S + \beta_3 \times \log L + \beta_4 \times \log R \tag{7}$$

where a and b are the intercept and slope of Power-law model. T, S, L and R represent the temperature, stress level, loading duration and rest ratio respectively. In addition, $\alpha_i$andβ_i are the regression constants.

Minimum least square method was used to obtain the coefficients of Power-law model. This method indicates that the coefficients (i.e. a_1, a_2,..., a_n) should be calculated for a given set of data $((x_1,y_1),(x_2,y_2),\ldots\ldots,(x_n,y_n))$ with respect to $y = f(a_1,a_2,\ldots,a_m, x)$. The Sum of Squared Errors (SSE), which presented in Eq. (8), should be minimized. Therefore, the best model that can be fitted to data is determined by calculating coefficients regarding the minimum SSE. Accordingly, the predictive model was presented in Table 7.

$$SSE = \sum_{i=1}^{n}(y_i - f_i)^2 = \sum_{i=1}^{n}(y_i - f(a_1, a_2, \ldots, a_m, x_i))^2 \tag{8}$$

where y_i is the i^{th} value of the variable to be predicted, x_i is the i^{th} value of the explanatory variable, f_i is the predicted value of y_i and a_1, a_2, ……,a_m are the coefficients of regressed model.

Generally, by adding an intercept to a main equation with a format of $y = f(x)$, the surface moves toward the vertical direction. However, it is expected that the newest equation should be more accurate than the previous one.

In this research, the overall format of the intercept equation is modified using an additional parameters (a_0). The developed model are presented in Table 7. According to this table, R-squared value is equal to 0.8772. It is clear that among different parameters, temperature has the greatest influence on the intercept and slope, whilst the loading duration applies the lowest

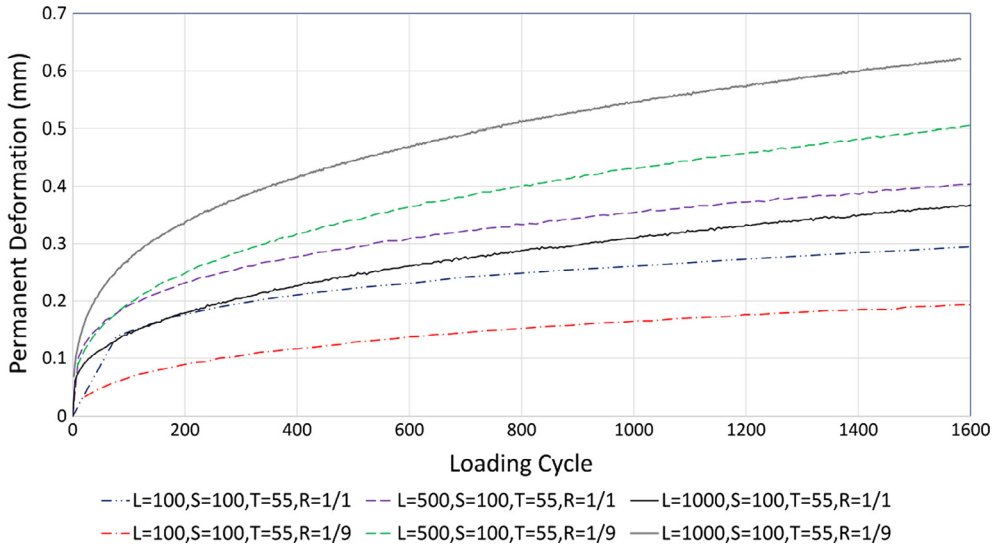

Fig. 6. Permanent deformation behaviour of HMA under different loading patterns.

Table 7
Permanent deformation models.

	Equation	R^2
Overall model	$\varepsilon = a \times N^b$	–
Primary developed model	$a = 0.6768 \times T^{-1.4968} \times S^{0.2834} \times L^{0.1788} \times R^{0.5692}$ $b = -2.2616 + 0.3256 \times \log S + 0.033 \times \log L - 0.1274 \log R + 1.1036 \times \log T$	0.8772
Modified model	$a = -0.1207 + 0.0957 \times T^{0.1593} \times S^{-0.0495} \times L^{0.000291} \times R^{0.1647}$ $b = -1.3416 + 0.3532 \times \log S + 0.4401 \times \log L + 0.0842 \times \log R - 0.1522 \times \log T$	0.956

effects. It is worth noting that the difference between obtained and predicted values should be small and unbiased (i.e. higher R-squared values desirable). It can be observed from Table 7 that the R-squared of the modified model (R^2=95.6%) is higher than primary model. Therefore, it can be said that the modified model is more accurate. Regarding the modified model, rest period and loading duration are the parameters that can considerably affect the intercept and slope, respectively. In fact, rest period is the most effective parameter that can affect the intercept equation. Nevertheless, this parameter have slight impact on slope equation. In addition, impact of loading duration on these parameters are vice versa. This could show that the impacts of different testing parameters on the permanent deformation behaviour depend on the model type that employed to analyse the experimental data.

According to the modified model, since the loading duration coefficient is very low (i.e. close to zero), the effect of this parameter on the intercept is inconsiderable. Furthermore, the highest coefficient of intercept is belonged to temperature parameter. This could indicate that the increment of testing temperature leads to a growth in the intercept. However, because of the negative coefficient of temperature in slope equation ((b) equation in modified model), higher temperatures lead to lower slope.

Moreover, axial deviator stress has a significant effect on the slope equation. If the test conditions are kept fixed and stress level is considered as a variation of model, the form of intercept equation is transformed as Eq. (9).

$$a = a_0 + \alpha \frac{1}{S^{0.0495}} \tag{9}$$

where a_0 and α are the intercept and slope, respectively; S is independent and a is dependent variables.

According to this Equation, it can be seen that higher amounts of stress level lead to a decrease in the intercept of the Power-law model. This trend continues until the intercept reaches a constant value. This shows that higher axial stress levels could have a negligible effect on the intercept. Nevertheless, this impact on the slope of the Power-law model is different. From slope equation (b) of modified model that mentioned in Table 7, it can be understood that greater stress level leads to an increase in slope equation. At initial loading cycles, different stress levels cannot significantly affect the permanent deformation behaviour, but at higher numbers of loading cycles, their impacts are more obvious. It was also found that an increase in rest period and loading duration result in higher permanent deformations. Although, the rest period coefficient in slope equation has the smallest magnitude, an increase in rest period duration leads to higher amounts of permanent deformation. Additionally, higher amount of loading duration can increase the observed permanent deformation.

In order to assess the validity of the generated model, the experimental data were compared with the predictive results (Fig. 7). Furthermore, the deviation distribution between experimental and predicted data is presented in Fig. 8. Whereas the amounts of deviation between observed and predicted data are presented in Fig. 9. This Figure illustrates that the average deviation between predictive and experimental data is equal to

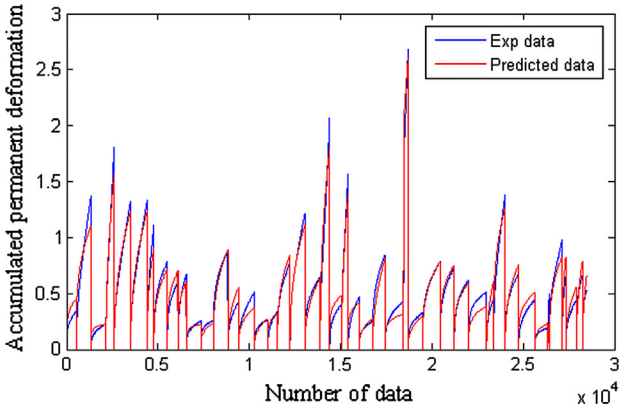

Fig. 7. Comparison between measured and predicted data.

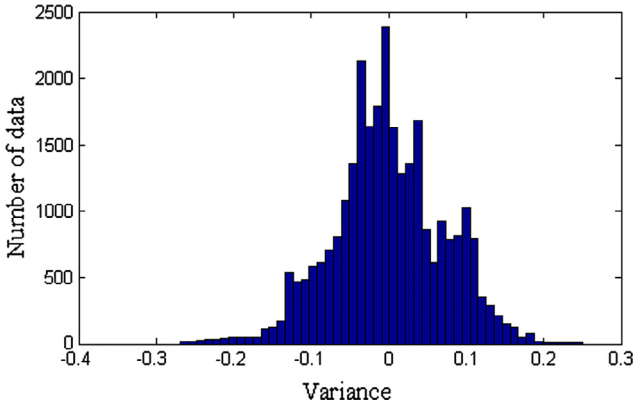

Fig. 8. Variance distribution between predicted and measured data.

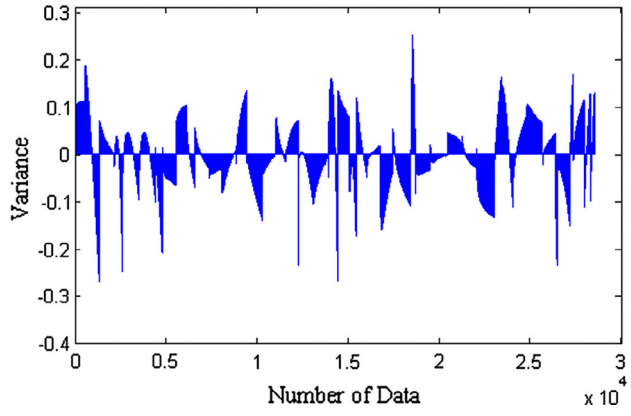

Fig. 9. Deviation between experimental and predictive data.

661.3 με. According to Fig. 7, the predicted and measured data are relatively close to each other. Regarding Figs. 8 and 9, it can be clearly seen that the variance between predicted and measured data are very small. Thus, it can be concluded that the modified developed model can be used to predict the permanent deformation behaviour in asphalt mixtures.

The sensitivity analysis of the predictive model has been carried out to determine its most effective parameters. In this respect, Figs. 10–12 show a comparison between predicted slopes and intercepts regarding the different combinations of the test parameters. It can be seen that the fifth order polynomial-exponential model is fitted to the predicted results of (a) and (b). These figures

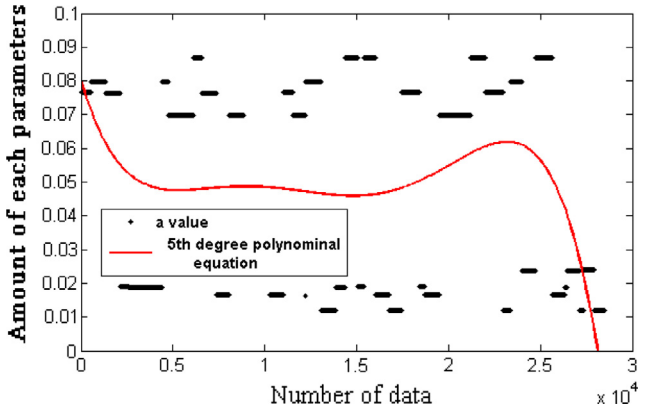

Fig. 10. 5th order polynomial - exponential fitted equation on "a" data.

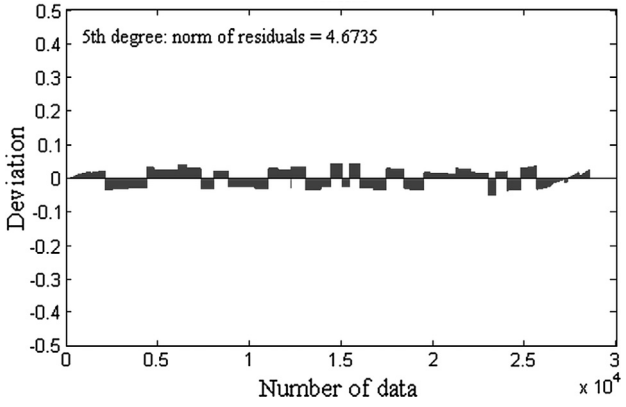

Fig. 11. Norm of residuals of intercept equation.

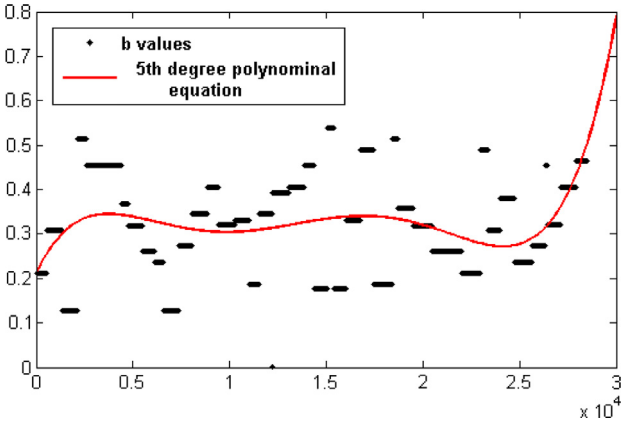

Fig. 12. 5th order polynomial - exponential fitted equation to "b" data.

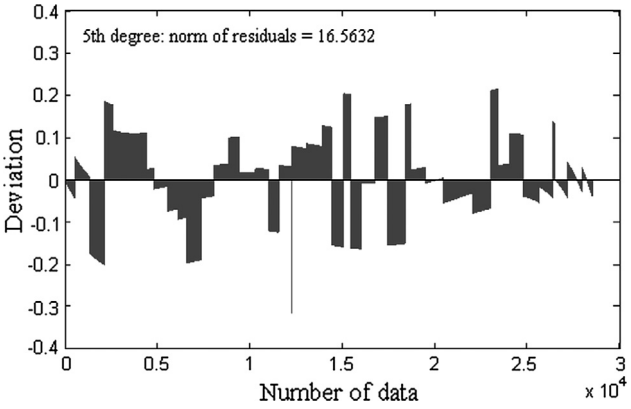

Fig. 13. Norm of residuals of slope equation.

represent the behaviour and sensitivity of the intercept and slope with respect to the different experimental conditions. Generally, (a) values tends linearly and it can be divided into two different categories. However, (b) changes sinusoidal with respect to different loading combinations. In addition, the intercept is more limited than the slope, and the slope is the most effective parameter in the predictive model. In other words, the slope of Power-law model is more influential than its intercept. Furthermore, the Norm of residuals was used as goodness of fit indicator. This indicator is a measure of the deviation between the correlation and the data (i.e. a lower norm signifies a better fitting). Figs. 11 and 13 indicated that the equations of the predictive model are fitted satisfactorily. This shows that the slope of Power-law model is more sensitive to variation of experimental parameters compared to the intercept. As mentioned previously, loading duration and axial stress level have the highest impacts on the slope equation respectively. Based on the developed predictive model, it can be understood that the permanent deformation in asphalt mixtures under cyclic loading is more sensitive to loading duration and axial stress level than testing temperature and rest time.

5. Conclusions

The main aim of this research was to develop a predictive model based on the results of RLPD test. Additionally, the impact of different experimental parameters on the permanent deformation of HMA was analysed. The most important findings are presented below:

1- The predictive model can be used successfully to predict the permanent deformation behaviour of asphalt mixtures under different loading combinations. In this regard, a traditional Power-law model was developed based on the experimental data with a suitable accuracy ($R^2 = 0.8772$). In addition, a modified Power-law model with a more accurate prediction has been presented ($R^2 = 0.956$).
2- It was found that the slope value (b) has more influence on permanent deformation than the intercept (a). Furthermore, regarding the developed model, the slope value was strongly depended on the loading duration and axial deviator stress.
3- One of the most effective parameters that can influence the permanent deformation behaviour in HMA was loading duration, followed by axial stress level and rest period duration. Longer rest period and loading duration lead to an increase in permanent deformation. The permanent deformations that occurred in the first zone are sensitive to rest period. However, the loading duration can affect the secondary zone of creep curve.

4- During the first zone of creep curve an increase in deviator stress level do not significantly affect the permanent deformation. However, during the secondary zone where the permanent deformations linearly increase, higher deviator stress level can increase the permanent deformations. Moreover, the testing temperature was one of the most effective parameters that can influence the permanent deformation performance in HMA.

References

[1] Y.H. Huang Pav. Anal. Des. 2003
[2] Y.R. Kim, Model Asph. Concr. (2009), https://doi.org/10.1036/007146462X.
[3] X. Qi, M. Witczak, Time-dependent permanent deformation models for asphaltic mixtures, Transp. Res. Rec. J. Transp. Res. Board. 1639 (1998) 83–93, https://doi.org/10.3141/1639-09.
[4] L. Mohammad, Z. Wu, S. Obulareddy, S. Cooper, C. Abadie, Permanent deformation analysis of hot-mix asphalt mixtures with simple performance tests and 2002 mechanistic-empirical pavement design software, Transp. Res. Rec. 2006 (1970) 133–142, https://doi.org/10.3141/1970-16.
[5] T. Xu, H. Wang, Z. Li, Y. Zhao, Evaluation of permanent deformation of asphalt mixtures using different laboratory performance tests, Constr. Build. Mater. 53 (2014) 561–567, https://doi.org/10.1016/j.conbuildmat.2013.12.015.
[6] G. Al-Khateeb, I. Basheer, A three-stage rutting model utilising rutting performance data from the Hamburg wheel-tracking device (WTD), Road Transp. Res. 18 (2009) 12–25.
[7] M. Ameri, M. Vamegh, R. Imaninasab, H. Rooholamini, Effect of nanoclay on performance of neat and SBS-modified bitumen and HMA, Pet. Sci. Technol. 34 (2016) 1091–1097, https://doi.org/10.1080/10916466.2016.1163394.
[8] F. Zhou, T. Scullion, L. Sun, Verification and modeling of three-stage permanent deformation behavior of asphalt mixes, J. Transp. Eng. 130 (2004) 486–494, https://doi.org/10.1061/(ASCE)0733-947X(2004) 130:4(486).
[9] M.W. Witczak, K. Kaloush, T. Pellinen, M. El-Basyouny, H. Von Quintus, Simple Performance Test for Superpave Mix Design (2002), https://doi.org/10.3141/1540-03.
[10] A. Bhasin, J.W. Button, A. Chowdhury, Evaluation of simple performance tests on hma mixtures from The South Central United States, Texas Transp. Inst. 9–5 (2004) 152.
[11] F. Zhou, T. Scullion, Preliminary field validation of simple performance tests for permanent deformation: case study, Transp. Res. Rec. 2003 (1832) 209–216, https://doi.org/10.3141/1832-25.
[12] M. Ameri, A.H. Sheikhmotevali, A. Fasihpour, Evaluation and comparison of flow number calculation methods, Road Mater. Pav. Des. 15 (2014) 182–206, https://doi.org/10.1080/14680629.2013.868819.
[13] H.U. Bahia, Ahmad F. Faheem, Hossein Ajideh, estimating the results of the proposed simple performance test for HMA from the Superpave Gyratory compactor results author, Transp. Res. Board. (2005) 1–25, https://doi.org/10.3141/1929-13.
[14] A. Kvasnak C.J. Robinette R.C. Williams, Statistical development of a flow number predictive equation for the mechanistic-empirical pavement design guide. Transportation research board 86th annual meeting. Transportation Research Board, 2007. pp. 18.
[15] S.W. Goh, Z. You, H. Wang, J. Mills-Beale, J. Ji, Determination of flow number in asphalt mixtures from deformation rate during secondary state, Transp. Res. Rec. J. Transp. Res. Board. 2210 (2011) 106–112, https://doi.org/10.3141/2210-12.
[16] C.L. Monismith, N. Ogawa, C.R. Freeme, Permanent deformation characteristics of subgrade soils due to repeated loading, Transp. Res. Rec. (1975) 1–17.
[17] L. Zhang, X. Zhang, C. Hu, Deformation prediction of asphalt mixtures under repeated load base on viscoelastic mechanical model, Paving Mater. Pav. Anal. (2010) 116–125, https://doi.org/10.1061/41104(377)15.
[18] G. Bernasconi, G. Piatti, Creep of Engineering Materials and Structures, Applied Science Publishers Ltd., London, 1978.
[19] M.A. Onyango, Verification of mechanistic prediction models for permanent deformation in asphalt mixes using accelerated, Pav. Test. (2009), https://doi.org/10.1007/s13398-014-0173-7.2.
[20] Witczak, M. W., and M. M. El-Basyouny. Appendix GG-1: Calibration of Permanent Deformation Models for Flexible Pavements. Guide for Mechanistic-Empirical Design of New and Rehabilitated Pavement Structures (2004).
[21] M.W. Witczak, R. Bonaquist, H. Von Quintus, K. Kaloush, Specimen geometry and aggregate size effects in uniaxial compression and constant height shear tests, J. Assoc. Asph. Paving Technol. 69 (2000) 733–793.
[22] M. Witczak C. Schwartz H. Von Quintus NCHRP Project 9-19: Superpave support and performance models management. Interim Report, Federal Highway Administration, National Cooperative Highway Research Program (2001).
[23] Witczak, Matthew W. Specification criteria for simple performance tests for rutting. Vol. 1. Transportation Research Board, (2007).
[24] W.J. Christopher, F.J. Crawford, T.H. Edward, M. Adock, E.P. Delaney, H. Freer, A Manual for Design of Hot Mix Asphalt with Commentary. NCHRP Report No. 673, (2011).
[25] Von Quintus, Harold L. Calibration of rutting models for structural and mix design. Vol. 719. Transportation Research Board, (2012).
[26] K.E. Kaloush, Simple performance test for permanent deformation evaluation of asphalt mixtures, Sixth Int. RILEM Symp. Perform. Test. Eval. Bitum. Mater. (2003) 498–505, https://doi.org/10.1617/2912143772.062.
[27] K. Biligiri, K. Kaloush, M. Mamlouk, M. Witczak, Rational modeling of tertiary flow for asphalt mixtures, Transp. Res. Rec. 2007 (2001) 63–72, https://doi.org/10.3141/2001-08.
[28] M. Ameri, A. Mansourian, A.H. Sheikhmotevali, Laboratory evaluation of ethylene vinyl acetate modified bitumens and mixtures based upon performance related parameters, Constr. Build. Mater. 40 (2013) 438–447, https://doi.org/10.1016/j.conbuildmat.2012.09.109.
[29] Standard, Australian. AS 2891.12. 1-1995: Methods of sampling and testing asphalt, method 12.1: Determination of the permanent compressive strain characteristics of asphalt-dynamic creep test. Standards Australia, Sydney. New South Wales, Australia (1995).
[30] Standard, British. Method for determining Resistance to Permanent Deformation of Bituminous Mixtures Subject to Unconfined Dynamic Loading. Draft for development, DD226, no. 1 (1996).
[31] Mansourkhaki, Ali, Alireza Sarkar. Plastic deformation of asphalt mixture under waveform loading. In Proceedings of the Institution of Civil Engineers-Transport, vol. 168, no. 3, pp. 200–211. Thomas Telford Ltd., 2015.
[32] F. Zhou T. Scullion, Vesys5 rutting model calibrations with local accelerated pavement test data and associated implementation (No. FHWA/TX-03/9-1502-01-2,). Texas Transportation Institute, Texas A & M University System. (2002). http://d2dtl5nnlpfr0r.cloudfront.net/tti.tamu.edu/documents/9-1502-01-2.pdf.
[33] Richard D. Barksdale, Laboratory evaluation of rutting in base course materials. In Presented at the Third International Conference on the Structural Design of Asphalt Pavements, Grosvenor House, Park Lane, London, England, Sept. 11–15, 1972., vol. 1, no. Proceeding. 1972.
[34] W.J. Kenis, Predictive Design Procedures. VESYS Users Manual. Report No. FHWA A-RD-77-154, Federal Highway Administration, (1977).
[35] Bayomy, Fouad Mohamed Sayed. Development and analysis of a cement coating technique: an approach toward distress minimization and failure delay in flexible pavements. (1983) 1561–1561.
[36] Kuo-Hung Tseng Robert L. Lytton Prediction of permanent deformation in flexible pavement materials. In Implication of aggregates in the design, construction, and performance of flexible pavements. ASTM International, (1989).
[37] M.W. Witczak, Development of the 2002 guide for the design of new and rehabilitated pavements-flexible pavements overview. Hot topics (2001).
[38] A.R. Archilla, L.G. Diaz, S.H. Carpenter, Proposed method to determine the flow number from laboratory axial repeated loading tests in bituminous mixtures, J. Transp. Eng. (2007) 610–617.
[39] Q. Li, H.J. Lee, E.Y. Hwang, Characterization of permanent deformation of asphalt mixtures based on shear properties, Transp. Res. Rec. 2181 (2010) 1–10.
[40] Iran Highway Asphalt Paving Code, Publication No. 234 Ministry of Road and Transportation Research and Education Center, Iran, 2003.
[41] ASTM D 1559-89. Test method for resistance to plastic flow of bituminous mixtures using Marshall apparatus. ASTM International, 1989.